Systems Code Analysis of HELIAS-type Fusion Reactor and Economic Comparison to Tokamaks

F. Warmer, S.B. Torrisi, C.D. Beidler, A. Dinklage, Y. Feng, J. Geiger, F. Schauer, Y. Turkin, R. Wolf, P. Xanthopoulos
Max Planck Institute for Plasma Physics
D-17491, Greifswald, Germany

R. Kemp, P. Knight, H. Lux, D. Ward
Culham Centre for Fusion Energy
Oxfordshire, OX14 3DB, United Kingdom

Contact: Felix.Warmer@ipp.mpg.de

***Abstract*— Systems codes are commonly employed for the analysis and conceptual design of fusion reactors. For the helical-axis advanced stellarator (HELIAS) line a new set of systems code models have been developed to account for the stellarator-specific 3D aspects. The models have recently been implemented in the systems code PROCESS and verified with respect to different test cases.**

After having established confidence in the stellarator models, systems studies were carried out for the 5-field period HELIAS case to define the accessible reactor design window. In the multi-dimensional physics and engineering parameter space sensitivity studies are carried out for the reactor regime to ascertain trade-offs between different parameters and costs. Exemplary design points are analysed in more detail using the plasma operation contour approach which, for example, can be used to determine the optimum start-up path to ignition.

Finally, with a common set of non-device-specific models, the PROCESS framework allows a direct comparison of tokamaks and stellarators. Although the 5-period HELIAS is a larger machine in terms of major radius, the required mass for both concepts is comparable leading to similar construction costs.

Keywords—Helical-Axis Advanced Stellarator (HELIAS), PROCESS, Systems Code, tokamak-stellarator comparison

I. INTRODUCTION

For an assessment of next-step fusion devices, it is not only important to find realistic design points consistent in physics and engineering but also to optimize these design points with respect to the high-level goals and costs. Furthermore, in such a conceptual design phase it is essential to show the robustness of design points with respect to variations in the underlying assumptions. Such a design process is commonly referred to as 'systems studies' where engineering and physics parameters are varied to define the accessible reactor design window and to study the sensitivity of the reactor regime considering trade-offs between important parameters and costs.

Such an approach has the advantage of revealing ambiguities in the underlying assumptions. These can then be clarified in dedicated experiments and simulations, thus defining a critical research path. Consequently, risks and uncertainties are mitigated before the actual engineering design process is started, thereby saving resources which would otherwise be needed for design iterations.

In order to carry out systems studies for next-step fusion devices associated 'systems codes' are used which are simplified, yet comprehensive models of an entire fusion power plant. Such an ansatz is commonly applied in the tokamak community, especially with respect to the assessment of a tokamak demonstration fusion power plant, also known as 'DEMO' [1]. Considering helical confinement concepts, similar studies have been done for the heliotron concept [2] and compact stellarators [3]. For the helical-axis advanced stellarator line (HELIAS), results of such a study are presented in this work for the first time.

For this purpose HELIAS-specific models have been developed [4]. These models include:

- First, a geometry model to describe the plasma shape (flux surfaces) based on Fourier coefficients. In position-space the geometry is described by cylindrical coordinates, which have been decomposed in a Fourier series allowing modeling of any arbitrary 3D toroidal surface. Such a formulation allows one to accurately calculate the important geometrical parameters such as plasma volume, surface area and cross-section which have direct impact on e.g. fusion power or neutron wall load. Moreover, it is possible to scale both the minor and major plasma radius by scaling of the corresponding Fourier coefficients making the model very flexible and suitable for a systems code approach.
- Second, a basic island divertor model for the energy exhaust was derived from geometrical considerations, in addition assuming cross-field transport and radiation at the X-point. The model is of analytic nature and combines physics and engineering relations. From the engineering side, the length of the divertor plate is estimated by considering how a helical field line in the scrape-off layer just passes the divertor plate on the inner side and the field line which hits the divertor on the outer side where the radial distance is given by the

size of the magnetic island. The broadening of the heat along such a field line is estimated by assuming diffusive cross field transport where the time it takes to reach the divertor is determined by the connection length.

- And third, a coil model which calculates the maximum field at the coils, the total stored magnetic energy, and the dimensions of the winding pack based on the sophisticated HELIAS 5-B [5] engineering design. For this purpose scaling relations and analytic inductance and field calculations are employed in combination with a critical current density scaling of the superconducting material used, i.e. scalings for both NbTi and Nb_3Sn have been implemented.

For the plasma transport, an empirical confinement time scaling is used. For stellarators, the most recent scaling is the so-called ISS04 scaling which was derived from the international stellarator-heliotron confinement database [6]. In such an ansatz, it is common to include a 'confinement enhancement factor' which describes the envisaged improvement of the confinement with respect to the empirical scaling. To improve the predictive capability of the confinement properties, transport simulations (including neoclassical and turbulent contributions) have been done [7]. The results of the transport simulations have been used to define the confinement enhancement factor for the studies presented here.

These models were implemented in the systems code PROCESS [8] which is a well-established, partly modular, European tokamak systems code which has gained maturity through years of applications. After the successful implementation, a verification study was carried out, in detail described in [9]. W7-X was modeled within the stellarator representation of PROCESS and compared to the real machine parameters. This comparison showed good agreement of the important parameters with maximum 10% deviation providing confidence for the use of the models for HELIAS systems studies. Their implementation in the original tokamak-centric code PROCESS has the additional advantage that the tokamak and stellarator concept can be compared within a common framework.

This work is divided into two parts. The first part, section II, is dedicated to HELIAS systems studies with emphasis on the general design window analysis and plasma operation contour analysis as well as specific examples such as the effect of tungsten impurities on start-up and plasma operation. The second part, presented in section III, makes use of the aforementioned common PROCESS framework (version 389) to compare exemplary tokamak and stellarator design points. Finally, the work is summarized and the results discussed in section IV.

II. HELIAS Systems Studies

A. Design Constraints and Goals

Before a design window of a HELIAS power plant type device can be outlined several general assumptions must be made about the constraints and goals of such a device. As the stellarator is intrinsically designed for steady-state operation, a HELIAS power plant aims for an economic base-load power output which must be at least comparable to the level of existing large power plants. Here, this is formulated as a constraint to achieve ~1GW net electric power. The production of net electric power is closely interconnected to two other systems of a fusion power plant, namely the power conversion system as well as the blanket structure. Both systems must be conceptually specified for a HELIAS systems analysis.

The power conversion system of thermal to electric energy is mainly dependent on the chosen coolant which determines the thermal conversion efficiency η_{th}. Common technologies employ either pressurized water or gaseous helium cooling. Water cooling is a well established technology requiring a moderate amount of pumping power but has a lower efficiency compared to helium. In turn, helium cooling requires a much higher pumping power. A detailed discussion of the advantages and disadvantages of both systems is still ongoing in the fusion community. In this work, the Brayton power cycle with helium cooling technology has been chosen for the cooling system due to the possibility of working at higher temperatures and avoiding the unresolved safety issues regarding water cooling [10]. Additionally, the higher thermal conversion efficiency, η_{th} = 0.4, compensates for the higher pumping power, P_{pump} = 200MW, assumed throughout this work [11, 12].

Several different technologies also exist for the blanket composition and its structure. It is beyond the scope of this work to compare the different blanket possibilities and benefits and drawbacks. For this work the dual-coolant (helium and lithium-lead) ferritic steel modular blanket concept was chosen described in [11] compatible with the outlined power conversion system above. This choice has been made here in order to facilitate the comparison to a tokamak. The in- and outboard thicknesses are summarized in Tab. 1, where the full blanket thickness is assumed everywhere to ensure a high tritium breeding ratio (TBR) for self-sustained tritium supply.

It should be noted that the application of these technologies do not represent a final decision but are chosen for a realistic representation of a HELIAS power plant. A decision about the heat conversion and blanket system can only be made after the experimental testing of blanket technologies and detailed assessment of the cooling systems. In fact, the European helium cooled pebble bed (HCPB) blanket design [12] seems more favorable for a stellarator due to the low space requirements. A detailed neutronics analysis of a HELIAS power reactor is ongoing [13].

TABLE I. Main design parameters assumed for the HELIAS systems studies unless otherwise stated.

Main design parameters	
Thermal efficiency for He-cooling η_{th}	0.4
Pumping Power for He-cooling [MW]	200
Inboard blanket thickness [m]	0.7
Inboard shield thickness [m]	0.4
Outboard blanket thickness [m]	0.8
Outboard shield thickness [m]	0.7
Superconducting Material	Nb_3Sn
HELIAS Field Periods	5
Number of Coils	50

In order to have enough space between the plasma and the coils to accommodate the specified blanket a higher aspect ratio of A = 12.2 has been chosen compared to the aspect ratio of A = 10.5 in W7-X [15]. The modular coil design and its cross-section are based on [16] where Nb_3Sn is used as superconducting material reflecting the experience gained from ITER.

This work concentrates on a HELIAS magnetic configuration with 5 field periods due to the more favorable physics properties, including better confinement of fast particles and reduced bootstrap current. A more compact 4-field-period device with lower aspect ratio may be of interest in future studies.

Empirical confinement time scalings have been widely used in the fusion community to assess and predict the confinement time τ_E in terms of global physics and engineering parameters. However, it was shown in [7] that an empirical scaling is not sufficient to predict the confinement properties of 5-field period HELIAS since results from detailed transport simulations deviate from the scaling at reactor-relevant parameters.

Although modern stellarators, like W7-X, are optimized for reduced neoclassical transport, the improvement of the global confinement by such measures remains to be proven. First indications, however, could be obtained by analyzing the dataset of the ISS04 scaling. Different devices, and even different magnetic configurations of the same device, are displaced with regard to the overall regression. Indeed, different clusters have been identified within the dataset used for the ISS04 scaling [6]. Consequently, a configuration-dependent factor, f_{ren}, has been introduced to account for a general improvement or degradation with respect to the reference scaling which is defined as $\tau_E = f_{ren} \cdot \tau_E^{ISS04}$. The renormalization factor f_{ren} can thus serve as a measure for the optimization of the magnetic configuration. The function of the renormalization factor is similar to the H-factor used in tokamaks. However, as described above, the underlying concept is quite different.

Transport codes can be employed to calculate the neoclassical and anomalous transport for a specific magnetic configuration to obtain a predictive confinement time [17]. Comparing the confinement time obtained from such simulations to the value given by the direct extrapolation of the ISS04-scaling allows one to obtain a predictive renormalization factor. For this reason, the renormalization factor is taken here to be synonymous with a confinement enhancement factor.

The transport simulations have been applied to a HELIAS reactor scenario and iterated back and forth with the systems codes studies. For conservative reactor parameters a maximum confinement enhancement factor of $f_{ren} = \tau_E / \tau_E^{ISS04} \leq 1.5$ was found [7] and serves as the upper limit for the present studies. According to the 1-D transport simulations with dominating neoclassical transport in the plasma centre and anomalous transport at the plasma edge the volume averaged temperature has been fixed for the HELIAS reactor studies to $\langle T \rangle_V$ = 7keV. The density on the other hand is iterated in the design window analysis to achieve the desired goals such as 1GW net electric power.

Stellarators are not subject to a density limit of the Greenwald type [18] and the radiative density limit, i.e. SUDO-limit [19], observed in some heliotron/stellarator-type devices is not considered in this work since the Large Helical Device (LHD) has demonstrated the ability to operate far beyond this limit, especially if pellet injection is used. Therefore the SUDO-limit has been reinterpreted as a density limit for the plasma edge [20, 21]. For the 5-field period HELIAS the SUDO-limit yields a value of $1.6 \cdot 10^{20} m^{-3}$ which is very high for an edge-limit and thus not relevant for the design window analysis considered here.

Another important aspect of a fusion power plant is the controlled exhaust of energy and particles through the divertor. The model of the island divertor concept consists of a geometrical description including cross-field diffusion and radiation in the SOL and around the X-point [4, 9, 22]. In order to model the island divertor, a set of assumptions is needed: For the SOL a perpendicular heat diffusion coefficient of $\chi = 1.5 m^2/s$ has been chosen from experimental experience. The inclination between field lines and the divertor target plates was selected to be $\alpha_{lim} = 2°$ with a field line pitch angle $\Theta = O(10^{-3})$. The temperature in front of divertor is estimated to be T_t = 3eV with an effective charge of Z_{eff} = 3 due to the radiating impurities. A heat load limit of $q < 5 MW/m^2$ is expected for steady-state reactor conditions [23]. In the following the radiation fraction in the SOL, f_{rad}*, is varied to stay within the heat load limit and serves as a figure of merit for the exhaust challenge.

As the scenarios investigated in this work concern a burning plasma with production of alpha-particles, helium dilution of the plasma must be taken into account. In order to estimate the helium 'ash' in the plasma, first a source profile has been defined by taking the alpha particle birth profile and assuming slowing down on the flux surface (i.e. neglecting losses of alpha particles). Secondly, using the neoclassical transport approach as discussed before, the particle flux of the helium ash is calculated and in combination with the source profile a helium density profile is obtained. This leads to a concentration of 10% helium 'ash' in the plasma. This cannot be ignored as helium dilution reduces the fusion power output. Apart from helium no further impurities have been taken into account for the plasma core. Only in the dedicated sensitivity study in section II.D have intrinsic tungsten impurities been considered. In future studies other seeded impurities may be taken into account to increase the radiation in the plasma core reducing the power crossing the separatrix and therefore easing the exhaust scenario.

B. Design Window Analysis

Design window analysis has originally been carried out for heliotron reactors as described in [24]. The aim of such an analysis is to define the accessible engineering and physics parameter range for a fusion power plant device respecting specified constraints and goals as described above. For this purpose the main engineering parameters of a HELIAS power plant (the major radius and the magnetic field strength on axis) were systematically varied within a reasonable range ($18m < R < 24m$; $4.5T < B_t < 5.6T$). In this study the high-level goals were kept constant. That means, in every design point a net

electric power of 1GW should be reached. To achieve this while varying the machine size and magnetic field, the plasma density and the confinement enhancement factor were iterated (subject to the limit obtained from the transport simulations).

Two cases are presented in the following, called (A) and (B). In the first case (A) the design window analysis is presented according to the assumptions and goals outlined above. In case (B) the helium ash concentration in the plasma is assumed to be 5% compared to the 10% in case (A) in order to assess the impact of helium dilution on the design window.

It should be noted that a single run of a stellarator scenario in PROCESS takes a few minutes on a modern computer. The total calculation time of a 2D-scan as presented in the following is therefore dependent on the chosen resolution. For the design window analysis a 16 x 16 resolution was chosen which corresponds to ~1 day of calculation time per figure [25].

1) Case (A)

The results of case (A) are shown in Fig. 1 where isocountours of the volume-averaged plasma beta and the averaged neutron wall load are used as limitations to the design window.

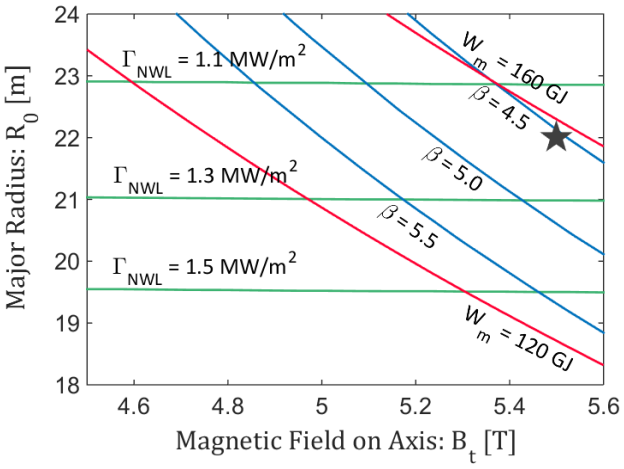

Fig. 1. Case (A): Design window for a HELIAS power plant device with 10% helium ash concentration constrained to achieve $P_{net,el}$ = 1 GW showing isocontours of the volume-averaged thermal plasma β (blue), the average neutron wall-load (green), and the stored magnetic energy (red).

An upper bound on the stored magnetic energy of W_{mag} = 160GJ was selected in accordance with [5] in order to keep the stress to components moderate, i.e. to stay below the typical stress limit for steel of 750MPa [16]. The average neutron wall load in this analysis is not a limiting factor. At a machine size of R = 23m the average neutron wall load is rather moderate with 1.1MW/m^2. A reduction of the machine size from 23m to 21m would increase the average neutron wall load by 20% which is still about a factor two lower than in a tokamak reactor [26]. However, the plasma beta (blue lines) is a limiting factor in the design window analysis. A conservative beta-limit of 4.5% as predicted by linear stability would lead to a narrow accessible reactor design range. But stellarator experiments have demonstrated the capability to operate above this limit [27, 28, 29, 30] such that beta may be ultimately limited by stochastisation of the plasma edge and corresponding destruction of flux surfaces resulting in a shrinking of the plasma volume. Such a beta-limit has been predicted to be in the range of 5 - 6% [29]. As shown in the figure an increase of beta from 4.5 to 5.5% would expand the available design window. A broader design window allows more freedom to choose a robust design point and further optimize the device with respect to costs, e.g. going to smaller field or machine size for cost reduction.

As already stated, the confinement enhancement factor has been iterated to be in line with [7]. For clarity, the associated isocontours of f_{ren} are illustrated separately in Fig. 2. In addition, the radiation fraction, f_{rad}*, which is needed to achieve a peak heat load limit of 5MW/m^2 on the divertor plates, is given in percent of the power crossing the separatrix.

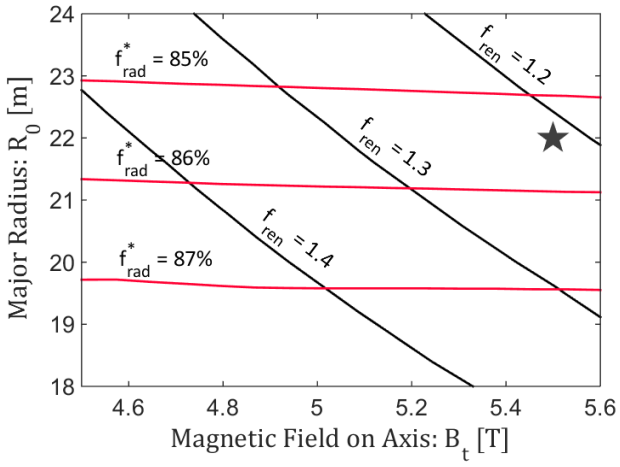

Fig. 2. Case (A): Complement to the design window for a HELIAS power plant device with 10% helium ash concentration constrained to achieve $P_{net,el}$ = 1 GW showing isocontours of the confinement enhancement factor f_{ren} (black) and the radiation fraction of the power crossing the separatrix to keep the peak heat load on the divertor plates at 5 MW/m^2 (red).

As can be seen in the complementary Fig. 2 the confinement enhancement factor is conservatively chosen for large machine sizes on the order of f_{ren} ~ 1.2 and increasing for smaller device sizes up to 1.4. The required radiation fraction varies only slightly between 85% - 87%. This is clear as in this design window the net electric power was fixed and thus the alpha heating power and consequently the power crossing the separatrix is nearly constant. Moreover the effective wetted area scales linearly with the major radius and thus changes only from A_{eff} = 12m^2 for the smallest device up to 15m^2 for the maximum size. It should be noted that a change of the radiation fraction of 1% is in this case equivalent to an additional power of 5MW going directly to the divertor.

2) Case (B)

The design window analysis for Case (B) is shown in Fig. 3. The contours of the neutron average wall load do not change in comparison to case (A) as the same fusion power is required to achieve 1GW net electric power and consequently, the neutron production stays the same. The β-contours on the other hand shift by about 1m to smaller device sizes and show the impact of the helium ash dilution on the plasma performance. A higher helium concentration in the plasma 'costs' beta and electron density without increasing the performance of the device.

A complementary figure with contours of the required radiation fraction and the confinement enhancement factor for case (B) is not shown as these parameters are similar to the results presented for case (A), Fig. 2.

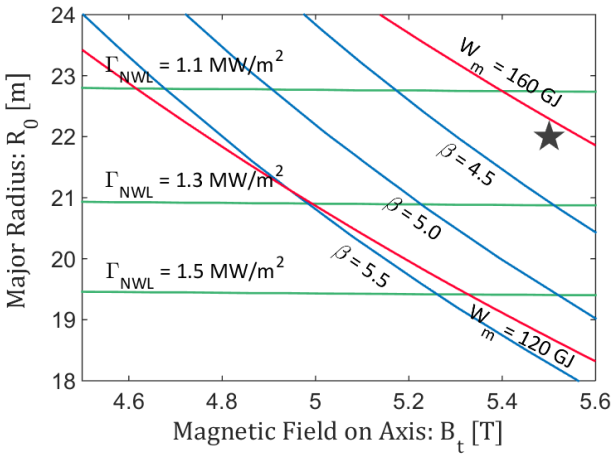

Fig. 3. Case (B): Design window for a HELIAS power plant device with 5% helium ash concentration constrained to achieve $P_{net,el}$ = 1 GW showing isocontours of the volume-averaged thermal plasma β (blue), the average neutron wall-load (green), and the stored magnetic energy (red).

If an operation scenario can be found which effectively flushs out the helium ash while keeping the confinement for the background plasma high, the size of the machine could be reduced to achieve the same power output or the power output can be increased for the same device size. E.g. if the density profile could be sufficiently controlled one could create a centrally hollow density profile. As the core transport in a stellarator is assumed to be dominated by neoclassical transport, the ambipolarity constraint would give rise to a positive electric field in the plasma centre [32] potentially increasing helium and impurity transport. The development and test of advanced scenarios is an ongoing research topic.

Another option are advanced quasi-isodynamic configurations with poloidally closed contours of B which are stable up to β = 7 – 8%. However, the design of a suitable coil set for such configurations remains a challenge.

C. Plasma Operation Contour Analysis

In the previous section a design window analysis of the HELIAS was carried out in which every point corresponded to a full reactor concept. Once a suitable design point is found through such a study, it is of interest to further investigate its properties and performance. This can be done by applying the methodology of Plasma Operation Contour Analysis [33] where density and temperature are varied and the external heating power is iterated to reach power balance.

As an example, such a study is presented in the following for the design point with R = 22m, B_t = 5.5T, and a confinement enhancement factor of f_{ren} = 1.2 lying well within the conservative accessible design window outlined by Fig. 1. The volume averaged temperature $\langle T \rangle_V$ and density $\langle n \rangle_V$ has been varied between 3 - 10keV and 0.3 - $3 \cdot 10^{20}$m^{-3}, respectively. The associated core radiation is assumed to be mainly bremsstrahlung and synchrotron radiation. Only for the tungsten case in section II.D is additional charge-state-averaged line radiation included. The results are illustrated in Fig. 4 where isocontours of the external heating power are shown. The heating power is required to balance the power loss through transport and radiation.

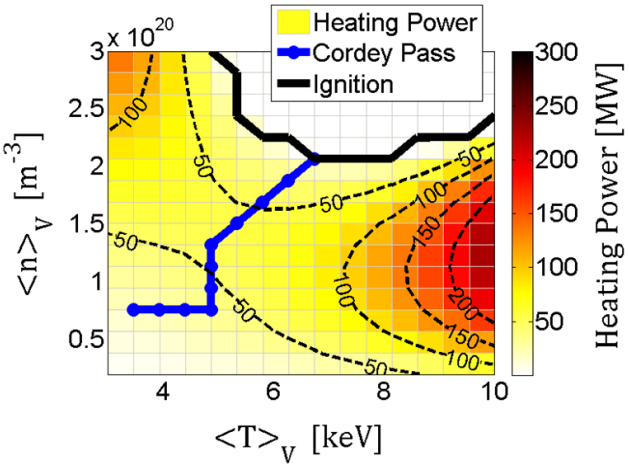

Fig. 4. Plasma Operation Contour Analysis (POPCON) for a HELIAS power plant design point with R = 22 m, BT = 5.5 T, 10% helium ash concentration, and f_{ren} = 1.2. Shown in colour-code and isocontours are the external heating power and in blue the Cordey-Pass to the ignition regime (white area).

As is well known and can be seen in Fig. 4, a 'valley' of minimum external heating power exists. This valley represents the optimum start-up path considering the minimisation for external heating power reserves. This optimum path is illustrated by a blue line and commonly referred to as the 'Cordey-Pass'. This path ends when the ignition region is reached where the plasma is self-sustained by the alpha heating power, shown as the white region with the black line serving as boundary.

A closer look at this Cordey-Pass can be taken by projection of the associated powers along the steps of this path, illustrated in Fig. 5. Shown are the increasing alpha heating and the increasing radiation while going in the

direction of start-up as well as the required external heating power which in this case has a maximum at 55MW. That means, that the minimum required heating power (MRHP) of 55MW must be available to achieve plasma start-up.

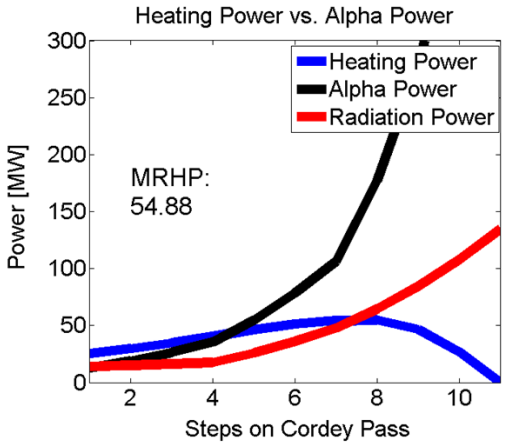

Fig. 5. Projection of the Cordey-Pass from Fig. 4 along its 'steps'. Shown are the external heating power (blue), alpha heating power (black), and the radiation loss power (red) along this path to ignition with a maximum required heating power of about 55 MW.

POPCON plots give insight into the performance of a single design point and the projection of the associated Cordey-Pass allows assessment of the required heating power for start-up. Even for the conservative HELIAS design point investigated here a self-sustained ignition window emerges which can be reached by applying 55MW external heating power during start-up.

D. Plasma Operation Sensitivity

Beyond the standard approach to POPCON plots, this methodology can be used for sensitivity studies of a design point against variations in different physics parameters. In the following the influence of two parameters on the plasma performance is studied.

The first parameter is the confinement enhancement factor. An improvement of the confinement leads to a reduction of power loss through transport if the plasma energy is to be kept constant. Consequently, this leads to a reduction of the required heating power as a smaller power loss must be compensated. Secondly, the impact of tungsten impurities on the plasma performance is investigated. This is important as a divertor must consist of a resilient material to sustain the strong heat loads. Currently, tungsten is discussed as a promising candidate which will be employed in ITER. But the bombardment of a tungsten metal divertor with energetic particles leads to sputtering and thus tungsten could be an intrinsic impurity in a reactor scenario.

The exemplary design point with R = 22m and B_t = 5.5T is considered for two different confinement enhancement factors, namely f_{ren} = 1.2 (top row) as well as f_{ren} = 1.4 (bottom row) as illustrated in Fig. 6. Also the tungsten concentration is changed from $c_W = 0$ (left column) to $c_W = 10^{-5}$ (right column).

As can be seen from Fig. 7 a moderate increase of confinement not only reduces the required external heating power to reach ignition but also generally increases the whole ignition parameter regime. A self-sustained ignition state is therefore reached at lower temperatures and densities. For the left side without tungsten impurities the required external heating power is reduced from 55MW to 20MW for an increase of the confinement enhancement from 1.2 to 1.4.

If now a moderate tungsten contamination is considered, the required external heating power strongly increases compared with the case without tungsten such that in the low-confinement scenario the ignition regime nearly vanishes in the considered parameter region. In this case the required heating power rises to a value of 120MW while in the high-confinement case the increase to 50MW is more tolerable. A closer comparison of the case with and without tungsten impurities also reveals that the impact of the tungsten contamination is greatest in the low temperature regime while the high temperature regime is nearly unchanged. This becomes clear when the radiative loss function of tungsten is examined which has a strong maximum at 2keV, see Fig. 6.

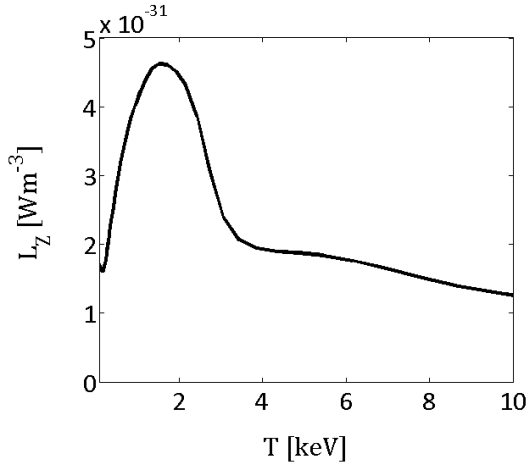

Fig. 6. Charge state averaged radiative loss function of tungsten in the relevant core-plasma temperature range.

From these results it can be concluded that the plasma must be kept free of highly radiating impurities during start-up in order to minimise the required external heating power. In the ignition phase, in contrast, a moderate concentration of impurities such as tungsten is tolerable or even favorable. As long as the confinement is not degraded, an increase of the core radiation through impurities reduces the power flow to the SOL. Thus, less radiation is required in the SOL easing the exhaust scenario.

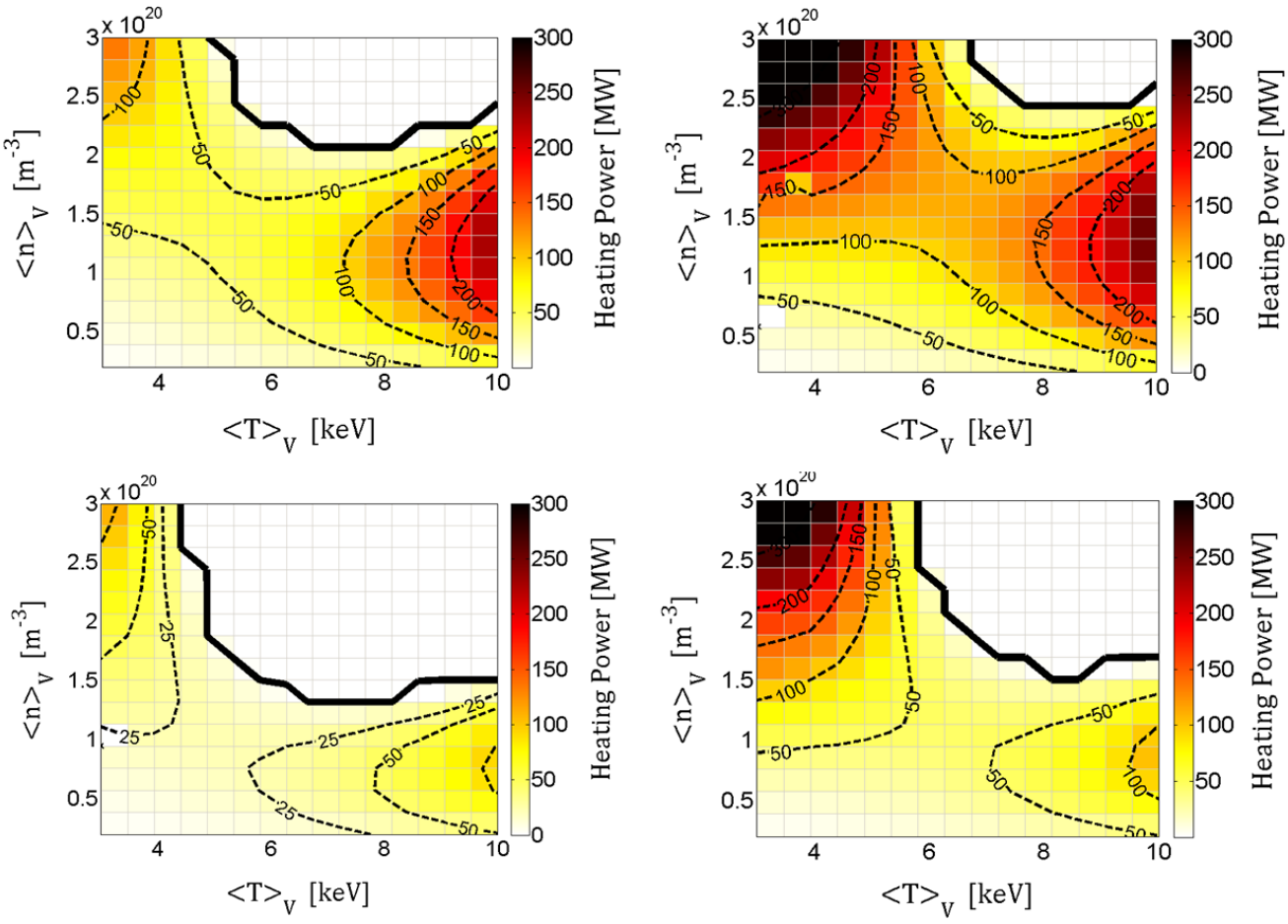

Fig. 7. Plasma operation contour plots are shown with isocontours for external heating power for a HELIAS scenario with R = 22 m, B_T = 5.5 T, 10% helium ash concentration, and a confinement renormalisation factor of 1.2 (top row) as well as 1.4 (bottom row). The left corresponds to cases without tungsten impurities in the plasma and the right to $c_W = 10^{-5}$.

III. Comparison to Tokamaks

A. Cost Assessment and Direct Comparison

In order to allow a comparison between tokamak and stellarator the same design goals and constraints, as outlined in section II.A, are applied to both concepts in the systems studies. In particular, the same blanket thickness has been taken for the tokamak case. Further, the tokamak H-factor has been used as iteration variable for the confinement enhancement similar to the renormalization factor used in stellarators. Current drive is employed to achieve steady-state operation of the tokamak in order to be comparable to the stellarator. The exhaust scenario, however, cannot be compared in this study as PROCESS currently does not feature a universally accepted tokamak divertor model.

Since every design point in the design window analysis represents a whole reactor design with hundreds of parameters, each point can be associated with corresponding construction costs. In a design point of PROCESS the size of each component is calculated. Each component is associated with a material or even a fractional composition of several materials. Based on the size of the components and the material densities the total weight for each material can be estimated. With a unit cost-per-weight the costs of each component are calculated. These are the direct costs of the device that are complemented by indirect costs which are in the current model simply a flat rate of the direct costs. The PROCESS cost model has been benchmarked with the dedicated cost analysis code FRESCO which showed a reasonable agreement for the total construction costs with deviations on the order of 20% [34].

In the following, exemplary design points are selected for both concepts and compared in a cost-breakdown. For the stellarator, the design point from section II.C is used with R = 22m, and B_t = 5.5T. For the tokamak a design point has been chosen which is similar to the 'Model B' of the European PPCS study [26]. This point lies in the middle of the PPCS parameter range and is therefore neither a too optimistic nor a too pessimistic design point with R = 8.5m, and B_t = 6T. The total construction cost of both these design points have been broken down to their major contributions, which are the magnets, the blanket, the buildings, the equipment and indirect costs, compared in Fig. 8.

A major contribution of the magnet costs is due to the coil conductors which are dominated by the high material costs for the superconductors (Nb_3Sn). A further cost driver of the magnets is the cost for assembly of such large coils. In total, the magnets contribute significantly to the total costs of a fusion power plant. It should be noted, that the 3D complexity of the stellarator will most likely increase the magnet costs, but this has not been taken into account here. However, while the modular coils of the HELIAS have about the size of the ITER TF-coils [5], the poloidal and toroidal field coils of the tokamak case are much larger. That means, while the HELIAS coils can still be produced by industry and shipped to the construction site, the tokamak coils must be built on-site. This requires a dedicated facility increasing the magnet costs for the tokamak, but which so far is also not taken into account. Thus arguments for cost increases can be found for both concepts and should be considered in future studies.

The blanket costs in this model are governed by the material costs for the breeder components. In addition, the large amount of steel required for the structural support and shield is a major contribution. The building costs reflect the high costs for both the reactor and turbine building. Additional building costs sum up all the smaller buildings which are required for the equipment, maintenance, etc. In this analysis the equipment costs themselves are also a major part of the total construction costs. This is clear as the equipment costs comprise several important reactor systems. Major contributions of the equipment costs come from the heating and fueling systems as well as from the cooling, cryogenic, and pumping systems and, last but not least, from the maintenance equipment and instrumentation and control. The last part in the construction costs are the so-called indirect costs. These are all costs which are not directly associated with a specific cost account, e.g. administration, safety, etc. These are assumed here to be a flat percentage of the direct costs.

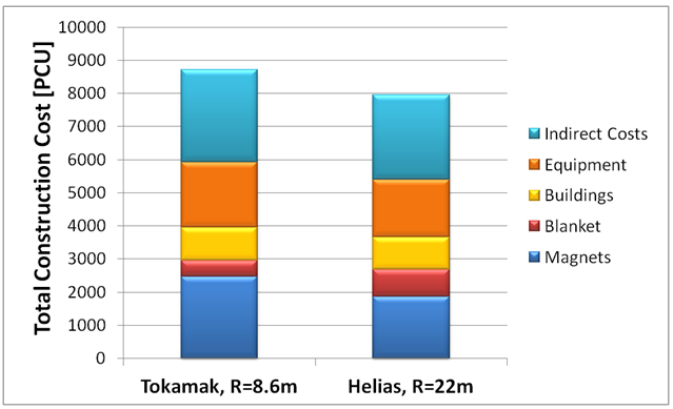

Fig. 8. Cost breakdown of total construction costs to major costing accounts for the selected tokamak and stellarator design point.

As can be seen from Fig. 8 and Tab. II the total magnet costs are higher for the tokamak than for the HELIAS as the massive PF coils and transformer add considerable mass of superconducting material (Nb_3Sn) and additional costs for assembly. The blanket costs on the other hand are higher for the HELIAS as the total surface area covered by the blanket is higher due to the higher aspect ratio. This in turn means also that the average neutron wall load is lower in the stellarator ensuring longer lifetime of the exposed inner components. The costs for the buildings are comparable in both the tokamak and stellarator case. The reactor building for the HELIAS must be broader but the tokamak reactor building on the other hand higher while the requirement for other buildings are similar. The equipment costs, in contrast, are higher for the tokamak as consequence of the requirement for external current drive.

TABLE II. COMPARISON OF RELEVANT PARAMETERS IN THE COST ASSESSMENT BETWEEN THE SELECTED TOKAMAK CASE AND THE HELIAS 5-B DESIGN POINT.

	Tokamak, R=8.6m	**Helias 5-B**
Fusion Power [GW]	3300	3000
Stored Magn. Energy [GJ]	170 (TF) + 20 (PF)	160
Vol. Averaged Plasma Beta [%]	4.3	4.4
Magnetic Field on Axis [T]	6.0	5.5
Av. Neutron Wall Load [MW/m²]	1.7	1.1
Cold Mass [kt]	43	40
Superconductor Mass (Nb_3Sn) [kt]	1.3	1.3

B. *Cost Sensitivity of Helias Reactor*

In order to further elucidate the construction costs of stellarator reactors, their sensitivity with respect to major engineering parameters shall be investigated in the following. Again, the design window analysis serves as basis for this study since each reactor design point can be associated with a detailed cost assessment. For this purpose, a range of isocontours for the total construction costs are illustrated in Fig. 9.

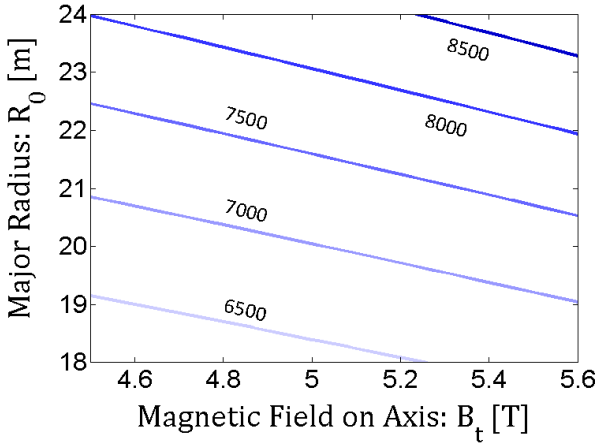

Fig. 9. Different isocontours of the total construction costs for the 5 field-period HELIAS design window analysis for a constant net electricity production of $P_{net,el}$ = 1 GW at constant aspect ratio, A = 12.2.

As can be derived from Fig. 9, the isocontours of the total construction costs are rather flat with respect to the investigated range of the magnetic field strength. Indeed, a reduction of the field from 5.5 to 4.5T on axis would reduce the total construction costs only by about 6-7% (for the same

superconductor material and for constant major radius and aspect ratio). The reduction of the field has mainly impact on the coil cross-section and thus on the total required superconductor mass and with the reduced field also on the required mass of support structure. While the magnet system becomes cheaper the costs for the blanket, buildings, and equipment remain the same, and consequently the reduction of the total construction costs is moderate. Decreasing the magnetic field seems therefore problematic as the reduction of the field would lead to a higher plasma beta if the fusion power is to be kept constant. This is in contradiction to the beta-limit discussed in Sec. II.B. On the other hand, a minimum plasma beta is required as the diamagnetic effect contributes to the confinement of the fast particles. Thus, operation at high beta is desirable from a physics point of view and economically meaningful. The confinement of the plasma is decreased, however, if the magnetic field strength is reduced. This means a higher confinement improvement of the configuration with respect to the ISS04 reference scaling is required in order to achieve the same power output.

Considering the major radius as an engineering parameter, the same cost saving of 6-7% can be achieved by reducing the major radius by about 1.5m (for constant magnetic field strength and aspect ratio). Therefore, reduction of the major radius provides more opportunity for cost savings. This is clear as the major radius has impact on all major components. The coils become smaller saving superconductor material. Further, the required support structure is reduced. In addition the surface area is reduced and with this the blanket and the associated breeder materials and steel. This in turn saves costs for cryogenic and pumping systems. Only the building costs remain constant as the reactor building is only slightly affected while the turbine building remains the same. The monetary gain by reduction of the major radius comes at the price of a higher neutron wall load and the requirement to go to a higher plasma beta (at constant fusion power). Thus, one may reverse the argument. Instead of focusing on cost reduction one can argue that by increasing the major radius by about 2m from 22 to 24m it is possible to strongly increase the fusion power output due to the increasing plasma volume while only moderately increasing the total construction costs by about 8-9%. As will be discussed below, an assessment of the cost-of-electricity is beyond the scope of this work, but the results presented in Fig. 9 suggest that a HELIAS reactor becomes more cost efficient at larger device sizes, which is also true for other toroidal reactor concepts.

Summarizing, the costs for a tokamak and a HELIAS reactor are comparable for the same set of goals in the common PROCESS framework with a simple cost model. Depending on which exact design points are compared construction costs can differ in the range of 10 – 20% for 'equivalent' assumptions. The cost-of-electricity (COE) is not investigated in this work. It was already shown in [33] that a variation and statistical sensitivity analysis of different cost factors leads to a non-uniform probability distribution of the COE where the COE with the maximum probability can significantly deviate from the reference value with fixed cost parameters. This is especially important as ambiguities regarding availability and maintenance time and costs exist which have a high impact on the COE. A detailed COE analysis is left for future studies once a better understanding of maintenance schemes is acquired.

IV. Conclusions

For the first time, a systems code approach has been applied to the helical-axis advanced stellarator line with the aim of defining the accessible design window for a power plant-sized-device. For this purpose, the major radius and the magnetic field on axis were varied over a wide range with the set goal to achieve 1GW net electric power. The results from the design window analysis have shown that the accessible design window depends strongly on the envisaged beta-limit. As the beta-limit for HELIAS devices has not yet been experimentally investigated one must await results from W7-X. The average neutron wall load on the other hand does not limit the design of a HELIAS as it does not exceed 1.5MW/m^2 even at smaller machine sizes due to the larger aspect ratio and surface area than typical for tokamak designs. The required confinement enhancement factor with respect to the ISS04 scaling lies between 1.2 - 1.3 for machines of every size at high field which is in line with results from detailed 1D transport simulations. In order to control the power exhaust of such a HELIAS device 85 - 87% of the total power must be radiated to ensure a peak heat load limit on the divertor targets of 5MW/m^2. In the plasma core, so far only bremsstrahlung and synchrotron radiation were considered, but additional power could potentially be radiated from the core if impurities were to be injected. Even under the most conservative assumptions with $\beta = 4.5\%$ and 10% helium concentration a feasible design window emerges around $R = 22$m, $B_t = 5.5$T. But if a scenario with effective helium ash exhaust can be found and/or the beta-limit can be verified to be higher, the design window notably increases opening many more options for potential devices and robust design points.

Beyond the design-window analysis, single design points were studied in more detail using plasma operation contour analysis. The start-up path to ignition was illustrated and it was shown that for a standard scenario about 55MW of external heating power are required. Furthermore, sensitivity studies were carried out varying the confinement enhancement and the tungsten impurity concentration. It became clear that a higher confinement strongly reduces the required external heating power while increasing the available ignition window. In contrast, an intrinsic impurity concentration of tungsten would make the start-up very difficult as tungsten has a strong radiation maximum at around 2keV while plasma operation at higher temperatures is not nearly so strongly affected.

Finally, the stellarator has been compared to the tokamak concept within the common PROCESS framework. A tokamak design point was studied for the same set of constraints and assumptions and the total construction costs compared. It is an important finding that the costs for a stellarator are on the same level as the costs for an equivalent tokamak. Although the stellarator is a larger machine in terms of its dimensions, the masses for the different components are comparable to those of a tokamak leading in this analysis to similar costs. A detailed cost break-down and comparison of a tokamak and stellarator

design point have shown that the costs of the tokamak magnet system are higher due to the high costs for the large PF and TF coils as well as the transformer. Also the equipment costs are higher in the tokamak case since the tokamak requires current drive to operate in steady-state which is more cost intensive and also decreases the net efficiency of the concept.

For the next steps, a detailed 3D neutronic analysis of the HELIAS concept has been started with the aim of defining and optimising a stellarator-specific breeder blanket. Moreover, systems and transport studies are being continued, which include in particular the concept development for a HELIAS burning plasma experiment.

ACKNOWLEDGMENT

Discussions with Prof. A. Sagara and Dr. T. Goto from the National Institute for Fusion Science, Japan, are greatly appreciated.

This work has been carried out within the framework of the EUROfusion Consortium and has received funding from the Euratom research and training programme 2014-2018 under grant agreement No 633053. The views and opinions expressed herein do not necessarily reflect those of the European Commission.

REFERENCES

[1] D. Maisonnier, D. Campbell, I. Cook et al. "Power plant conceptual studies in Europe" Nuclear Fusion, vol. 47, p. 1524 (2007).

[2] T. Goto, J. Miyazawa, H. Tamura et al. "Design Window Analysis for the Helical DEMO Reactor FFHR-d1" Plasma and Fusion Research: Regular Articles, vol. 7, p. 2405084 (2012).

[3] F. Najmabadi, A. R. Raffray, ARIES-CS Team "The ARIES-CS Compact Stellarator Fusion Power Plant" Fusion Science and Technology, vol. 54, p. 655 (2008).

[4] F. Warmer, C. D. Beidler, A. Dinklage et al. "HELIAS Module Development for Systems Codes." Fusion Engineering and Design, vol. 91, p. 60 (2014).

[5] F. Schauer, K. Egorov and V. Bykov. "HELIAS 5-B magnet system structure and maintenance concept." Fusion Engineering and Design, vol. 88, p. 1619 (2013).

[6] H. Yamada, J. H. Harris, A. Dinklage et al. "Characterization of energy confinement in net-current free plasmas using the extended International Stellarator Database." Nuclear Fusion, vol. 45, p. 1684 (2005).

[7] F. Warmer, C. D. Beidler, A. Dinklage et al. "Limits of Confinement Enhancement in Stellarators." Fusion Science and Technology, vol. 68, p. 727 (2015).

[8] M. Kovari, R. Kemp, H. Lux et al. "PROCESS: A systems code for fusion power plants - Part 1: Physics." Fusion Engineering and Design, vol. 89, p. 3054 (2014).

[9] F. Warmer, C. D. Beidler, A. Dinklage et al. "Implementation and Verification of a HELIAS module for the Systems Code PROCESS." Fusion Engineering and Design, vol. 98-99, p.2227 (2015).

[10] M. Tillack, P. Humrickhouse, S. Malang et al. "The use of water in a fusion power core." Fusion Engineering and Design, vol. 91, p. 52 (2015).

[11] A. R. Raffray, L. El-Guebaly, S. Malang et al. "Engineering Design and Analysis of the ARIES-CS Power Plant." Fusion Science and Technology, vol. 54, p. 725 (2008).

[12] U. Fischer, P. Pereslavtsev and S. Hermsmeyer. "Neutronic design optimisation of modular HCPB blankets for fusion power reactors" Fusion Engineering and Design, vol. 75-79, p. 751 (2005).

[13] A. Häussler, U. Fischer, F. Warmer. "Neutronics source modeling for stellarator power reactors of the HELIAS-type" submitted to the Proceedings of the Annual Meeting on Nuclear Technology (2016)

[14] H. Zohm. "On the minimum size of DEMO." Fusion Science and Technology, vol. 58, p. 613 (2010).

[15] G. Grieger and I. Milch. "Das Fusionsexperiment WENDELSTEIN 7-X." Physikalische Blätter, vol. 49, p. 1001 (1993).

[16] F. Schauer. "Coil winding pack FE-analysis for a HELIAS reactor." Fusion Engineering and Design, vol. 86, p. 636 (2011).

[17] Y. Turkin, C.D. Beidler, H. Maaßberg, et al. „Neoclassical transport simulations for stellarators" Physics of Plasmas, vol. 18, p. 022505 (2011).

[18] M. Greenwald, "Density limits in toroidal plasmas" Plasma Physics and Controlled Fusion, vol. 44 (2002)

[19] S. Sudo, Y. Takeiri, H. Zushi et al. "Scalings of energy confinement and density limit in stellarator/heliotron devices." Nuclear Fusion, vol. 30, p. 11 (1990).

[20] J. Miyazawa, R. Sakamoto, S. Masuzaki et al. "Density limit study focusing on the edge plasma parameters in LHD." Nuclear Fusion, vol. 48, p. 015003 (2008).

[21] L. Giannone, R. Burhenn, K. McCormick et al. "Radiation power profiles and density limit with a divertor in the W7-AS stellarator." Plasma Physics and Controlled Fusion, vol. 44, no. 10, p. 2149 (2002).

[22] Y. Feng. "Up-scaling the island divertor along the W7-stellarator line." Journal of Nuclear Materials, vol. 438, p. S497 (2013).

[23] H. Zohm, C. Angioni, E. Fable, et al. "On the physics guidelines for a tokamak DEMO" Nuclear Fusion, vol. 53, p. 073019 (3013).

[24] T. Goto, J. Miyazawa, H. Tamura et al. "Design Window Analysis for the Helical DEMO Reactor FFHR-d1." Plasma and Fusion Research: Regular Articles, vol. 7, p. 2405084 (2012).

[25] S. Torrisi and F. Warmer. "Design of an N-Dimensional Parameter Scanner for the Systems Code PROCESS." Report No. 13/23, Max-Planck-Institute for Plasma Physics (2014).

[26] D. Maisonnier, D. Campbell, I. Cook et al. "Power plant conceptual studies in Europe." Nuclear Fusion, vol. 47, p. 1524 (2007).

[27] H. Yamada, A. Komori, N. Ohyabu et al. "Configuration flexibility and extended regimes in Large Helical Device." Plasma Physics and Controlled Fusion, vol. 43, no. 12A, p. A55 (2001).

[28] A. Weller, J. Geiger, A. Werner et al. "Experiments close to the beta-limit in W7-AS." Plasma Physics and Controlled Fusion, vol. 45, no. 12A, p. A285 (2003).

[29] W. A. Cooper, L. Brocher, J. P. Graves et al. "Drift Stabilisation of Ballooning Modes in an Inward-Shifted LHD Configuration." Contributions to Plasma Physics, vol. 50, p. 713 (2010).

[30] K. Ichiguchi and B. A. Carreras. "Multi-scale MHD analysis incorporating pressure transport equation for beta-increasing LHD plasma." Nuclear Fusion, vol. 51, no. 5, p. 053021 (2011).

[31] M. Drevlak, D. Monticello and A. Reiman. "PIES free boundary stellarator equilibria with improved initial conditions." Nuclear Fusion, vol. 45, p. 731 (2005).

[32] F. Warmer. "Reactor Extrapolation of Wendelstein 7-X." Report No. 13/21, Max-Planck-Institute for Plasma Physics (2013).

[33] W. Houlberg, S. Attenberger and L. Hively. "Contour analysis of fusion reactor plasma performance." Nuclear Fusion, vol. 22, no. 7, p. 935 (1982).

[34] C. Bustreo, G. Casini, G. Zollino et al. "FRESCO, a simplified code for cost analysis of fusion power plants." Fusion Engineering and Design, vol. 88, no. 12, pp. 3141 (2013).

[35] C. Bustreo, T. Bolzonella and G. Zollino. "The Monte Carlo approach to the economics of a DEMO-like power plant." Fusion Engineering and Design, [in press], (2015).